Excimer Laser Ablation of Novel Triazene Polymers: Influence of Structural Parameters on the Ablation Characteristics

Th. Lippert,[†] J. Stebani,[‡] J. Ihlemann,[§] O. Nuyken,[‡,⊥] and A. Wokaun*,[†]

Physical Chemistry II and Macromolecular Chemistry I, University of Bayreuth, D-95440 Bayreuth, Germany, and Laser-Laboratorium Göttingen, D-37016 Göttingen, Germany

Received: May 5, 1993; In Final Form: September 20, 1993®

Novel photopolymers based on the triazene chromophoric group have been developed. Structuring by XeCl* excimer laser irradiation at 308 nm results in ablation craters with clean contours and sharp edges; diffraction-limited resolution of ≈0.4 μm is achieved. A prominent feature of the triazene polymers is the complete absence of solid debris around the edges of the ablation craters, which makes these materials attractive for applications in microelectronics. The dependence of the ablated depth per pulse on laser fluence is investigated and is related to the effective absorption coefficient and the quantum yield of photochemical decompostion of the polymers in solution. Other physicochemical and thermomechanical parameters of the polymers appear to be less influential on the ablation characteristics. The high fluence limit d_{max} of the etch rate per pulse is found in the range between 2 and 3 μm for all investigated materials. On exposure to several high fluence laser pulses, an ejection of material has been observed from areas that are considerably larger than the incident laser beam. This effect may be due to either an explosive event or the generation of shock waves reflected at the sample substrate.

Introduction

Recent years have seen the entry of laser system tools into materials processing. In polymer science, interesting technical applications such as cutting, boring, and microstructuring of synthetic fibers[1-7] have become accessible with the advent of high-energy pulsed excimer lasers. Excimer lasers have been successfully used in the structuring of photopolymers; particularly attractive is their application in the dry etching of resists in microlithography.[3,8]

The XeCl* excimer laser, which operates with He/Xe/HCl gas mixtures that are less toxic than the fluorine-based systems, offers the advantages of high pulse energies, long gas lifetimes, and low operational cost. However, only a few polymers can be ablated at the 308-nm wavelength, as a consequence of the lack of absorption of most polymers at this wavelength.[9,10] Two routes have been described that enable the application of XeCl* excimer lasers in polymer ablation. A first approach is the sensitization of non-absorbing polymers by physical doping with small concentrations of suitable chromophores.[11-13] A complementary route, which aims at the tailored synthesis of photopolymers containing a suitable chromophoric group, is the subject of the present study.

In a preliminary communication[14] on this project, three different polymers containing triazene chromophores have been tested for excimer laser ablation. A polycondensation product with two triazene groups per repeating unit (termed "TP2" in ref 14) was found to exhibit the best ablation characteristics.

In the present study, nine polymers have been synthesized by polycondensation of several different bis diazonium ions and diamino compounds. To obtain insight into the ablation mechanism, the ablation characteristics of these materials (threshold fluence, effective absorption coefficient, and maximum ablated depth per pulse) are compared with physicochemical parameters of the polymers, such as the glass transition and decomposition temperatures.

CHART I: Structural Formulas of Investigated Triazene Polymers

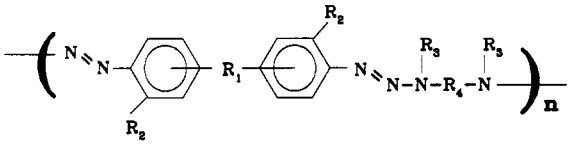

label	R_1	R_2	R_3	R_4
1[a]	O	H	CH_3	C_6H_{12}
2	O	H	CH_3	C_2H_4
3	-	OCH_3	CH_3	C_6H_{12}
4	p-SO_2[b]	H	CH_3	C_6H_{12}
5	m-SO_2[b]	H	CH_3	C_6H_{12}
6	CO	H	CH_3	C_6H_{12}
7	O	H	CH_3	C_3H_6
8	O	H	C_2H_5	$(CH_2-CH=)_2$
9	CO	H	C_2H_5	$(CH_2-CH=)_2$

[a] designated as TP 2 in Ref. 14

[b] the triazeno substituents are in meta- or para-position, respectively, with respect to the bridging SO_2 group

Experimental Section

Materials. The general structure of the materials synthesized is shown in Chart I. The individual polymers, as distinguished by the groups R_1 through R_4, are identified by labels in the caption, which will be used throughout the rest of the paper.

The polymers were synthesized according to the following general procedure. A bis(4-aminophenyl)ether, ketone, or sulfone (R_1 = O, CO, or SO_2, respectively, cf. Chart I) was diazotized with nitrite in hydrochloric acid. The bis diazonium product was not isolated, but a substituted diaminoalkane ($R_3NHC_nH_{2n}NHR_3$) was added to the solution, to yield the desired product in a polycondensation reaction. Details of the synthesis are described at another place.[15] The polymers obtained were purified by dissolution in tetrahydrofuran (THF) and reprecipitation by methanol addition. The materials were characterized by gel

* Author to whom correspondence should be addressed.
† Physical Chemistry II, University of Bayreuth.
‡ Macromolecular Chemistry I, University of Bayreuth.
§ Laser-Laboratorium Göttingen.
⊥ Present address: Institute of Technical Chemistry, Technical University of Munich, D-85748 Garching, Germany.
® Abstract published in *Advance ACS Abstracts,* November 1, 1993.

0022-3654/93/2097-12296$04.00/0

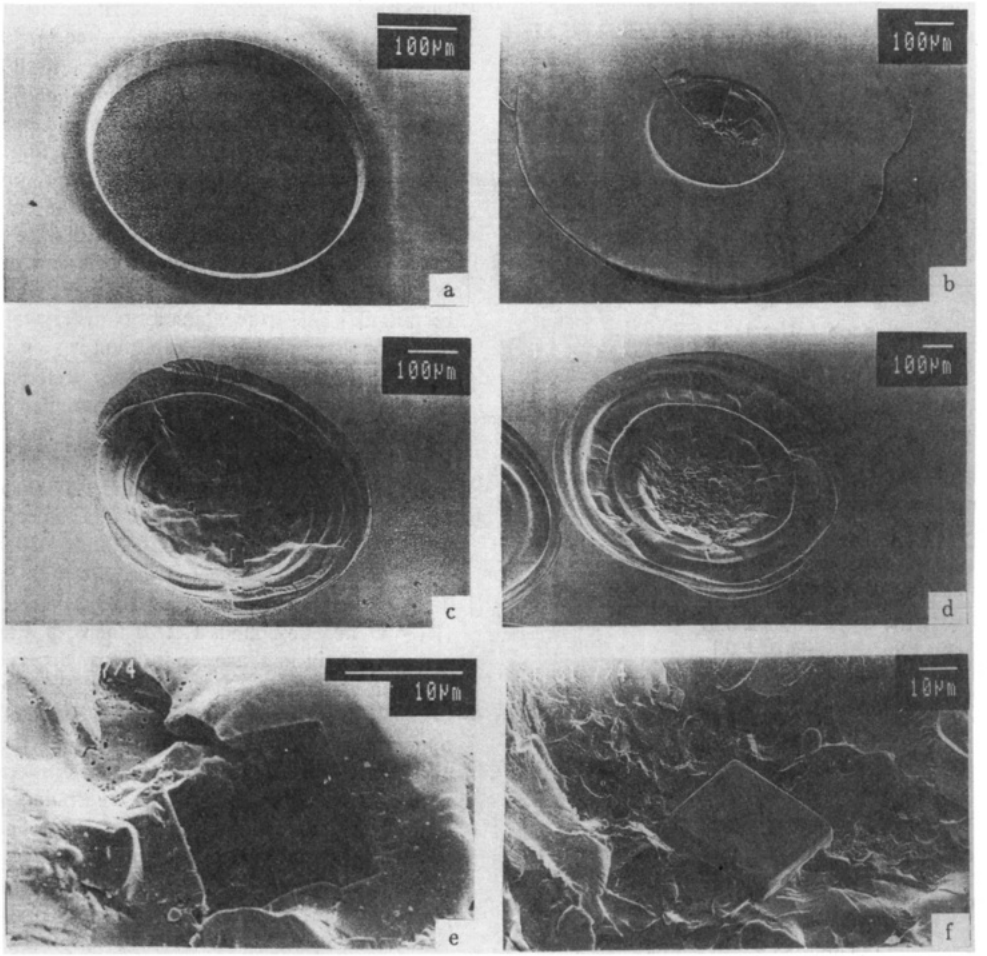

Figure 1. Scanning electron micrographs of ablation craters in triazene polymer **8**, produced by 308-nm excimer laser pulses incident on a 375-μm-diameter area on the sample: (a) 100 pulses of 1.2 J cm^{-2} fluence; (b) 2 pulses of 19 J cm^{-2} fluence; (c) 8 pulses of 6.6 J cm^{-2} fluence; (d) 2 pulses of 19 J cm^{-2} fluence; (e) details of a hole seen on the bottom of the crater shown in d; (f) details of a crystal seen on the bottom of the crater in d.

permeation chromatography (GPC), NMR spectroscopy, differential scanning calorimetry (DSC), and thermal gravimetric analysis (TGA). Selected results will be indicated below, while the full details of the characterization are reported in ref 15.

Preparation of Films. Polymer films were prepared by casting from THF solution onto glass substrates. The films were dried *in vacuo* (40 mbar) for 3 days at 40 °C. This procedure ensures that the solvent (boiling point 67 °C at ambient pressure) is largely removed from all polymers, including those with the lowest glass transition temperatures. Resulting film thicknesses were determined to lie in the 100–200-μm range.

Instruments. For the determination of ablation rates, irradiations were carried out with the experimental setup described in detail elsewhere.[12] Pulses from a XeCl* excimer laser (Lambda Physik, Model EMG 203 MSC, pulse duration ≈30 ns) were delivered to the sample at a rate of 2 Hz. The beam was apertured by a 3-mm circular diaphragm, which was imaged onto the sample surface using a 100-mm-focal length lens. A circular area of 375-μm diameter was homogeneously illuminated in this manner.

For the resolution tests, the same laser was used in combination with a different optical setup similar to the one described in ref 12b. A copper mask (source: Smethurst High-Light) with a rectangular slit, of 25-μm width, was imaged onto the sample surface using a Schwarzschild type reflecting objective (Ealing Electrooptics) with a demagnification ratio of 25:1 and a numerical aperture NA = 0.4. This objective, which was provided with a special coating for 308 nm, is virtually free of chromatic aberrations and offers the advantage of a large working distance (14.5 mm).

To realize ridges of varying width between the etched rectangular grooves, the sample was translated through a series of decreasing distances between the successive irradiations, by means of a stepper-motor driven translator.

Results

Ablation Profiles. Polymer **8** was chosen as a representative example to illustrate the morphologies resulting from excimer laser irradiation. A scanning electron micrograph of an ablation crater produced is shown in Figure 1a. The sample was irradiated with 100 pulses of 1.2 J cm^{-2} fluence at 308 nm. Corresponding well-defined profiles with perfectly circular contours are obtained for all investigated polymers. Similarly sharp contours had been found in our preliminary study[14] of triazene polymer **1**, which was designated as TP 2 in ref 14. This favorable behavior, which has rarely been observed with other materials, appears to be a unique property of the triazene polymers.

A striking feature that distinguishes the triazene polymers from other photosensitive materials used in laser ablation is the absence of ejected material deposited around the craters. A possible reason for the missing of solid ablation products, the so-called "debris", is the well-defined fragmentation of the polymer. Small gaseous molecules are resulting from the photodecomposition. These gaseous products, in particular N_2, are acting as a driving gas which promotes at least the initial stages of the ablation, thereby removing other polymer fragments from the surface.[12,13] In addition, thermal decomposition mechanisms may be important for high fluence pulses.

For all triazene polymers, the total ablated depth at a given fluence (laser pulse energy per irradiated area) increases linearly with the number of pulses. For the series of four polymers containing an oxygen bridge between the phenyl rings (R_1 = O

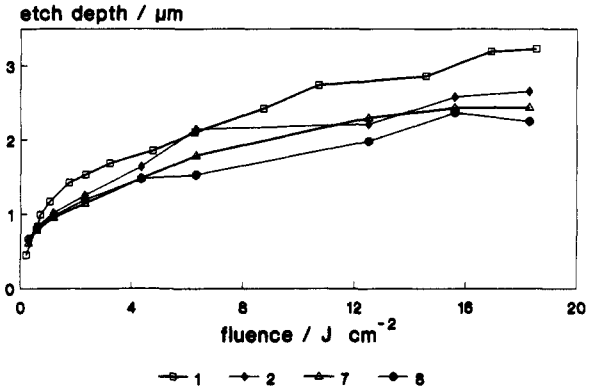

Figure 2. Dependence of the etch depth (ablated depth per pulse) on the laser fluence for polymers **1**, **2**, **7**, and **8** containing an oxygen bridge (R_1 = O in Chart I).

TABLE I: Parameters Characterizing Ablation of Investigated Polymers[a]

polymer label[b]	$d_{max}/\mu m$	F_0[c]/(mJ cm^{-2})	α_{eff}[c]/(10^4 cm^{-1})	$F_0\,\alpha_{eff}$/(kJ cm^{-3})
1	3.2	104	1.83 ± 0.03	2.1
2	2.6	96	2.20 ± 0.1	2.1
3	2.8	117	1.85 ± 0.06	2.2
4	2.6	104	2.19 ± 0.09	2.3
5	2.4	80	2.29 ± 0.1	1.8
6	2.5	106	2.37 ± 0.1	2.5
7	2.4	108	2.30 ± 0.2	2.5
8	2.2	54	2.58 ± 0.08	1.4
9	2.4	129	2.31 ± 0.14	3.0

[a] d_{max} = plateau etch depth; F_0 = threshold fluence; α_{eff} = absorption coefficient. [b] Cf. Chart I. [c] From a plot of low fluence etch rates versus ln F according to eq 1.

in Chart I), the increase of the ablated depth per pulse with laser fluence is shown in Figure 2. In the low-pulse energy regime, the fluence dependence is well represented by the equation[10]

$$d(F) = \frac{1}{\alpha_{eff}} \ln\left(\frac{F}{F_0}\right) \qquad (1)$$

where $d(F)$ is the ablated depth per pulse, F is the laser fluence, and F_0 represents the threshold fluence. The effective absorption coefficient for ablation, α_{eff}, is different from the linear absorption coefficient due to multiphoton and other effects, as has been pointed out in the literature.[16]

A plot of ablated depths per pulse for the low fluence regime according to eq 1 has been used to calculate the characteristic parameters, threshold fluence, and effective absorption coefficient, for the different polymers; results are collected in Table I.

For fluences exceeding a typical value of 1 J cm^{-2}, the rate of increase of $d(F)$ becomes more gradual than predicted by eq 1, until a plateau etch depth per pulse, d_{max}, is reached which cannot be exceeded in the range of fluences ≤20 J cm^{-2}. For each polymer, an average has been calculated from the three data points of depths ablated using fluences between 12 and 20 J cm^{-2} (cf. Figure 2); this average was included in Table I as a representative value for d_{max}.

An unusual and novel phenomenon was observed with some of the polymers upon irradiation with several pulses of higher fluences, as shown in the scanning electron images b–d of Figure 1. Micrographs c and d of Figure 1 exhibit ill-defined, deep craters, the sizes of which exceed the one of the laser beam by factors of ≈2–3 (note the calibration bars). There are several terraces or steps when processing from the circumference to the center. Such a massive ejection of material might be the result of a laser induced explosion[17] of the triazene polymer, which of course is accessible to thermal decomposition. Alternatively, the large crater might result from a shock wave[18] launched by the laser and reflected from the substrate. The latter mechanism is supported by micrograph b, where a large circular disk surrounded by a crack appears to have been lifted off the glass substrate.

The block-shaped objects discerned at the bottom of the craters in Figure 1c,d, and shown at a higher magnification in Figure 1f, have been identified as NaCl crystals, by means of energy dispersive X-ray analysis of the corresponding spot in the electron microscope. Apparently some sodium chloride resides within the material from the preparation of the polymer. [We recall that the triazene polymers were synthesized from a solution of the diazonium ion in 10% hydrochloric acid, to which an aqueous Na_2CO_3 solution is added subsequently.] A corresponding rectangular hole from which an NaCl crystal has been torn out of the polymer during the explosion is seen in micrograph e.

Physicochemical Characterization. Reference data from physicochemical characterization are compiled in Table II. The molecular weight M_w of the polymers was determined by gel permeation chromatography. For seven of the polymers, molecular weights between 50 000 and 120 000 were found. Compounds **7** and **8** are exceptional in this respect as their molecular weight is lower, i.e. between 10 000 and 20 000.

Results of thermogravimetric analysis are presented in Figure 3. The polymers with an oxygen bridge between the aryl moieties (R_1 = O, i.e. compounds **1**, **2**, **7**, and **8**; cf. Chart I) exhibit only a single weight loss, as seen in Figure 3a; its size indicates that nitrogen and the R_3–N–R_4–N–R_3 moiety are released in one step. With the other polymers, an ejection of nitrogen at lower temperatures followed by a the release of the bis(alkylamino)-alkyl fragment in a second step are observed [Figure 3b]. We note that, while the less stable triazene moiety decomposes always first in the slow thermal analysis scan, this sequence is not necessarily followed during the ultrafast photoablation process.

A GC/MS analysis of the thermolysis products has been performed. Products detected include unsubstituted and amino-substituted biphenyl ethers, radical coupling products containing two such units, and (dialkylamino)alkanes. All of these products are compatible with a radical decomposition mechanism, followed by release of nitrogen and radical recombination.

UV spectra in THF solution are presented in Figure 4 for two representative triazene polymers, **3** and **5**. The positions of the respective absorption maxima, together with the molar extinction coefficient at 308 nm relevant for the ablation experiments, are included in Table II for the entire series of compounds.

The THF solutions have been irradiated by excimer laser pulses at 308 nm, at a fluence of 50–60 mJ cm^{-2}. Changes in the UV spectra after a defined number of pulses were monitored, as illustrated in Figure 4. The principal absorption maximum is seen to decrease monotonically; analysis indicates that the decomposition proceeds to the products in a single-step reaction on the time scale of observation. Thus quantum yields of photolysis may be simply determined and were found in the range between 0.12 and 0.74%, as indicated in Table II. No dependence of the quantum yield on fluence was observed in the range between 30 and 70 mJ cm^{-2}.

Resolution Tests. The achievable resolution was tested for the material **1**, as described in the experimental part. A rectangular slit mask was imaged onto the sample, to illuminate a stripe of ≈1-µm width. The sample was irradiated with 10 pulses of 0.2 J cm^{-2} fluence and then translated in the focal plane prior to the next irradiation. The grooves produced by the photolytic decomposition are shown in Figure 5 at various magnifications. Again we note the exceptionally clean contours and the absence of any debris on the surrounding polymer surface. Particularly noteworthy are the sharp edges and the steep walls of the ridges, as displayed in the bottom micrograph of Figure 5.

For the imaging system used in our study (λ = 308 nm, numerical aperture NA = 0.4), the diffraction limited resolution $\lambda/(2NA)$ would amount to 0.385 µm. It has been pointed out in the literature (see, e.g. ref 19, and references cited therein)

TABLE II: Physicochemical Reference Data of Investigated Polymers[a]

polymer label[b]	M_w/ (g mol^{-1})	glass transition temp/K	decompsn temp/K	decompsn enthalpy/(kJ mol^{-1})	activation energies[c]/(kJ mol^{-1})	λ_{max}/nm	ϵ at 308 nm/ (M^{-1} cm^{-1})	photolysis quantum yield[d]/%
1	71 000	336	555	−255	211/203	330	27 700	0.26
2	46 000	357	549	−299	196/115	333	24 900	0.39
3	53 000	353	484/545[e]	−258	82/160	367	11 300	0.17
4	107 000	383	508/567[e]	−257	89/162	336	23 200	0.12
5	207 000	358	513/573[e]	−258	104/166	293	22 500	0.16
6	61 000	361	573	−255	149/182	352	17 200	0.13
7	19 000	341	548	−254	168/83	331	23 900	0.74
8	9 000	314	477	−253	120/138	334	22 400	0.64
9	69 000	348	484/541[f]	−351	137/178	357	18 400	0.16

[a] M_w = molecular weight; λ_{max} = absorption maximum; ϵ = extinction coefficient. [b] Cf. Chart I. [c] From a fit of the DSC curves according to a two-step kinetic model A → B → C. [d] In tetrahydrofuran solvent. [e] Shoulder. [f] Two resolved peaks.

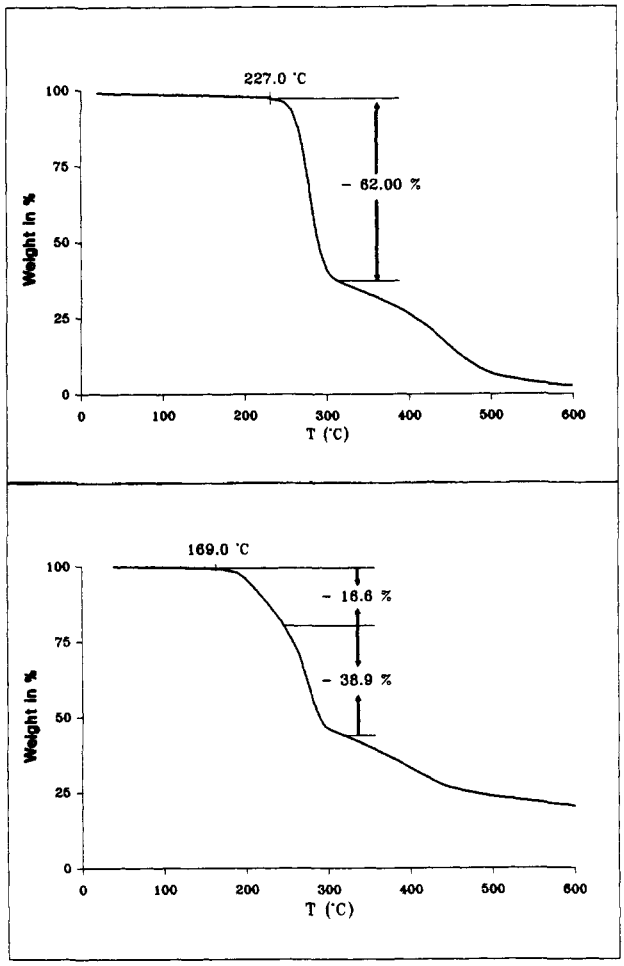

Figure 3. Thermogravimetric analysis of triazene polymer decomposition. A single weight loss is observed for materials with an oxygen bridge (R_1 = O), as shown in the upper panel for polymer **1**; two releases of matter are observed for the remaining materials investigated, as demonstrated in the lower panel for polymer **3**.

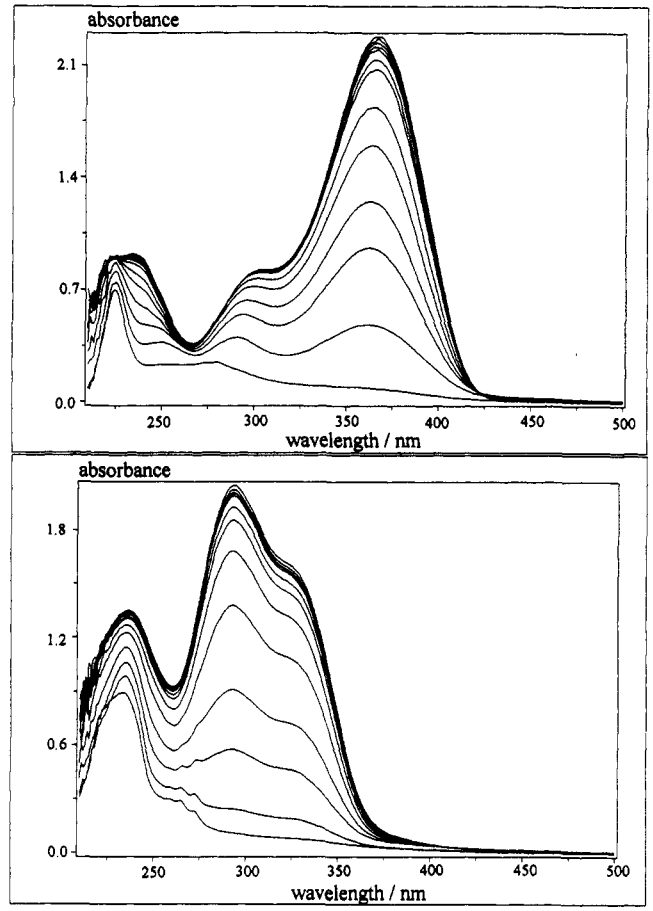

Figure 4. UV spectra and excimer laser photolysis in THF solution of the triazene polymers **3** (top) and **5** (bottom). In each diagram, the topmost trace represents the spectrum of the parent solution. Subsequent traces with decreasing absorption were recorded after 2, 5, 10, 15, 30, 50, 100, 150, 250, 350, 500, and 1000 (**3** only) excimer laser pulses at 308 nm had been delivered to the sample. The pulse energy was 114 mJ for **3** and 84 mJ for **5**, both times incident onto the 2-cm^2-area window of the quartz cuvette containing the sample solution.

that the resolution in photoablation can in fact exceed the diffraction limit, as a consequence of nonlinear effects. Judging from the sharpness of the contours seen in the micrographs of Figure 5, the resolution achieved corresponds at least to the diffraction limit, i.e. ≈0.4 μm. A more quantitative evaluation by atomic force microscopy is in progress.

Additional information on the wavelength dependence of ablation for polymer **1** is available in ref 14, where the fluence dependence of the etch rate has been reported for 248-nm irradiation.

Discussion

Ablation and Parameters from Thermal Analysis. There appears to be no obvious correlation between the ablation characteristics of the various polymers and the corresponding data from thermal analysis (Table II). A possible exception is polymer **8**, where low values of the glass transition and decomposition temperatures are associated with a low threshold fluence F_0 and a low maximum etch rate d_{max}. A plot of the plateau etch rates against decomposition temperature is presented in Figure 6. Apart from the materials **8** and possibly **9**, the two variables appear not to be correlated. We conclude that the thermal component of ablation does not represent the most influential factor for the ablation characteristics of the present systems.

The significance of the thermal analysis results with respect to structural and thermomechanical properties of the polymer materials will be discussed in more detail at another place.

Relations between Threshold Fluence, Effective Absorption Coefficient, and Maximum Etch Rate. The *low fluence* etch rates

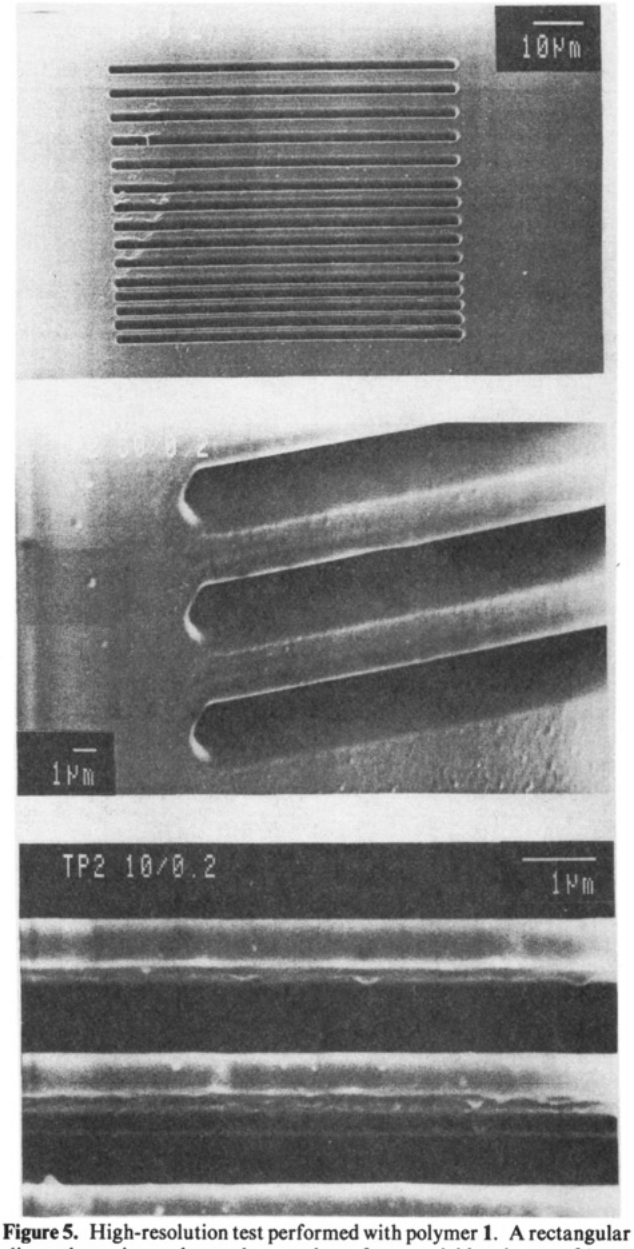

Figure 5. High-resolution test performed with polymer **1**. A rectangular slit mask was imaged onto the sample surface, to yield an image of 1-µm width and illuminated with 10 pulses of 0.2 J cm^{-2} fluence at 308 nm. Between successive series of 10 pulses each, the sample was translated by varying distances. The slots and ridges produced are shown at various magnifications, as identified by the calibration bars.

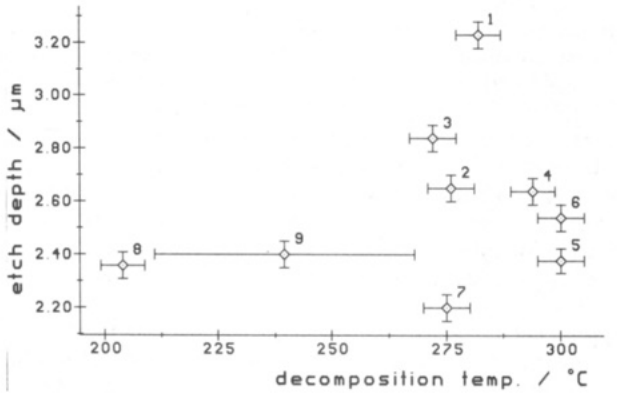

Figure 6. Plot of the high fluence etch depth, d_{max}, against the decomposition temperature T_d determined by differential scanning calorimetry. Polymers **1–9** are identified in Chart I.

have been analyzed by linear regression according to eq 1, and the effective absorption coefficient α_{eff} was determined from the

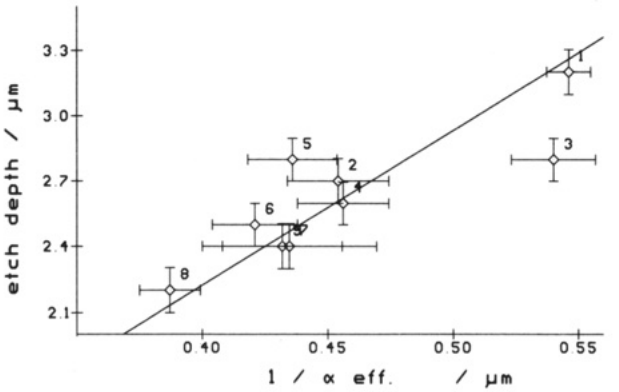

Figure 7. Correlation of the *high fluence* etch depth, d_{max}, with the inverse effective absorption coefficient $1/\alpha_{eff}$, determined from a regression analysis of *low fluence* data according to eq 1, as described in the text.

slope. As mentioned above, α_{eff} contains contributions from both linear and nonlinear effects. A clear linear correlation between the *high fluence* plateau etch rate, d_{max}, and the inverse effective absorption coefficient $1/\alpha_{eff}$ is demonstrated for all nine polymers in Figure 7. This result shows that the maximum ablated depth per pulse is limited by the same type of nonlinear processes for all investigated polymers, in spite of the fact that the absorption maximum varies from 293 nm for polymer **5** to 367 nm for polymer **3**.

The threshold fluence F_0 (Table I) is more or less constant (104 ± 25 mJ cm^{-2}). Polymer **8** represents again an exception with a remarkably low threshold fluence of 54 mJ cm^{-2}. When discussing the ablation mechanism, it is illuminating to consider the product $F_0\,\alpha_{eff}$, included in the last column of Table I. It has been pointed out[20] that, for a purely thermal ablation process, $F_0\,\alpha_{eff}$ should be constant within a series of comparable materials. Inspection of Table I reveals that this is not the case for our systems, which may be taken as another strong indication for the importance of the photochemical decomposition process described above.

Molar Extinction Coefficient and Quantum Yield of Decomposition at 308 nm. A common feature of the triazene polymers is the absence of any simple relation between the *effective* absorption coefficient obtained from the analysis of the ablation data and the molar absorption coefficient at 308 nm in solution. This lack of correlation is not unusual in polymer ablation[9] and has been ascribed to nonlinear effects (saturation of absorption, multiphoton excitation) and to absorptions by laser-induced plasma, photoproducts, and the ejected gas plume.[21] A recent study indicates the importance of the absorption by gaseous products.[22]

Indications for an influence of the quantum yield of photolysis at 308 nm in solution on the low fluence etch rates have previously been obtained by us for poly(methyl methacrylate) (PMMA) doped with molecular triazene chromophores.[13] To test for a possible influence of the solution quantum yield of the polymers (determined at 308 nm in tetrahydrofuran solution) on the ablation characteristics, the etch depth d_{max} was plotted against the quantum yield in Figure 8.

The etch depth is seen to increase with the quantum yield, as expected for a photochemical decomposition mechanism, for polymers **1**, **3–6**, and **9**. However, if we focus on the class of the four oxygen-bridged polymers **1**, **2**, **7**, and **8** (R_1 = O; cf. Chart I), an opposite correlation is observed in Figure 8: Within this subset, the polymers with the highest quantum yield are characterized by the lowest etch depth d_{max}.

From a chemical standpoint, it is anticipated that the electron-donating or withdrawing character of the bridging substituent R_1 would profoundly influence the decomposition behavior. A decrease of d_{max} with quantum yield, as found for the latter group of materials, would point to the importance of thermal energy

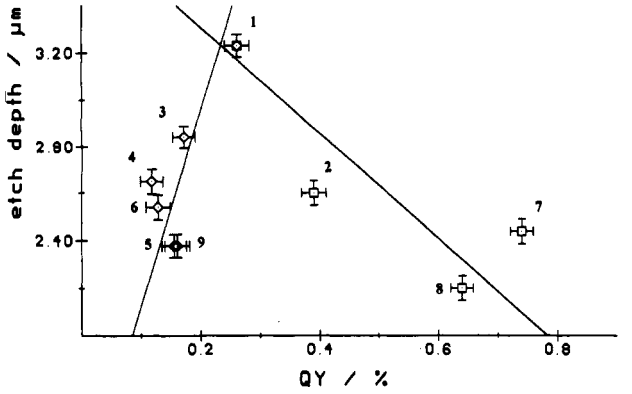

Figure 8. Correlation of the high fluence etch depth, d_{max}, with the photolysis quantum yield of the polymers at 308 nm, determined in tetrahydrofuran solution. The straight lines obtained by linear regression for two subsets of the data points are discussed in the text.

deposition in the high fluence regime, in line with the argument presented in ref 13: A triazene chromophore with a low photolysis quantum yield is capable of undergoing more cycles of photon absorption followed by thermalization, as compared to a material with a higher quantum yield of decomposition. Further experiments will be required to elucidate the origin of the described differences between the two groups of materials shown in Figure 8.

Conclusions

The ablation characteristics of the investigated triazene polymers appear to be determined by the main chain chromophoric groups. Thermal properties, such as the glass and decomposition temperatures, appear to be of lesser importance. This observation indicates that the ablation is governed by the photolytic decomposition of the triazene groups.

The effective absorption coefficient α_{eff} relevant for low fluence ablation is not simply related to the molar extinction coefficient in THF solution. Within a set of polymers with the same hexamethylene spacer R_4, but different bridging groups R_1, the maximum etch rate d_{max} increases with the photolysis quantum yield in solution (Figure 8). In contrast, an opposite correlation has been observed within the subset of oxygen bridged triazene polymers (R_1 = O).

A unique feature is the absence of solid polymer deposits around the ablation craters. This point is very relevant for applications in microelectronics. With other polymers tested in the literature, supplementary techniques are usually applied to prevent a contamination of the photolithography mask or of the polymer layer itself, such as electrostatic collection of the debris,[23] processing *in vacuo*[24] or in an oxygen atomsphere,[25] flood irradiation with additional pulses of lower fluence,[19] or use of a second IR laser.[26] The fact that solid debris is absent with the triazene polymers, which are quantitatively decomposed into volatile products upon photolysis, offers the important advantage that these supplementary measures are not required.

High-resolution tests performed with polymer **1** show that the developed materials may be suitable candidates for microlithography applications. Well-defined grooves with sharp edges and steep walls may be produced, without any debris being deposited on the surrounding polymer surface. The achievable resolution appears to be equal or better than ≈0.4 µm.

Acknowledgment. We are most grateful to J. Winkler, A. Lang, and J. Reiner for performing the GC/MS analysis of the products from thermal decomposition. Financial support of this work by grants of the Deutsche Forschungsgemeinschaft (SFB 213) and by the Verband der Chemischen Industrie is gratefully acknowledged.

References and Notes

(1) Srinivasan, R. *J. Vac. Sci. Technol.* **1983**, *B1*, 923.
(2) Deutsch, T. F.; Geis, M. W. *J. Appl. Phys.* **1983**, *54*, 7201.
(3) Rice, S.; Jain, K. *Appl. Phys.* **1984**, *A33*, 195.
(4) Dyer, P. E.; Sindhu, J. Opt. Lasers Eng. **1985**, *6*, 67.
(5) Jain, K. *Excimer Laser Lithography*; SPIE: Bellingham, WA, 1990.
(6) Bachmann, F. *Chemtronics* **1989**, *4*, 149.
(7) Bachmann, F. *MRS Bull.* **1989** (Dec), 49.
(8) Lankard, J. R., Sr.; Wolbold, G. *Appl. Phys.* **1992**, *A54*, 355.
(9) Lazare, S.; Granier, J. *Laser Chem.* **1989**, *10*, 25.
(10) Srinivasan, R.; Braren, B. *Chem. Rev.* **1989**, *89*, 1303.
(11) Srinivasan, R.; Braren, B.; Dreyfus, R. W.; Hadel, L.; Seeger, D. E. *J. Opt. Soc. Am.* **1986**, *B3*, 789.
(12) (a) Bolle, M.; Luther, K.; Troe, J.; Ihlemann, J.; Gerhardt, H. *Appl. Surf. Sci.* **1990**, *46*, 279. (b) Ihlemann, J.; Schmidt, H.; Wolff-Rottke, B. *Adv. Mater. Opt. Electron.* **1993**, *2*, 87.
(13) Lippert, T.; Stebani, J.; Ihlemann, J.; Nuyken, O.; Wokaun, A. *Angew. Makromol. Chem.*, in press.
(14) Lippert, T.; Wokaun, A.; Stebani, J.; Nuyken, O.; Ihlemann, J. *Angew. Makromol. Chem.* **1993**, *206*, 97.
(15) Stebani, J.; Nuyken, O.; Lippert, T.; Wokaun, A.; *Makromol. Chem. Rapid Commun.* **1993**, *14*, 365.
(16) Srinivasan, V.; Smrtic, M. A.; Babu, S. V. *J. Appl. Phys.* **1986**, *59*, 3861.
(17) Koren, G.; Oppenheim, U. P. *Appl. Phys.* **1987**, *B42*, 41.
(18) Zweig, A. D.; Deutsch, T. F. *Appl. Phys.* **1992**, *B54*, 76.
(19) Brannon, J. H. *J. Vac. Sci. Technol.* **1989**, *B7*, 1064.
(20) Fukumura, H.; Mitsuka, N.; Eura, S.; Masuhara, H. *Appl. Phys.* **1991**, *A53*, 255.
(21) Lazare, S.; Granier, V. *Chem. Phys. Lett.* **1990**, *168*, 593.
(22) Lazare, S.; Granier, V. *Appl. Phys. Lett.* **1989**, *54*, 862.
(23) von Gutfeld, R. J.; Srinivasan, R. *Appl. Phys. Lett.* **1987**, *51*, 15.
(24) Seeger, D. E.; Rosenfield, M. G. *J. Vac. Sci. Technol.* **1988**, *B6*, 399.
(25) Singleton, D. L.; Paraskevopoulos, G.; Irwin, R. S. *J. Appl. Phys.* **1989**, *66*, 3324.
(26) Koren, G.; Donelon, J. J. *Appl. Phys.* **1988**, *B45*, 45.